FULL PAPER

Dalton
www.rsc.org/dalton

Ionic multi-component complexes containing $TDAE^{\bullet+}$ and $C_{60}^{\bullet-}$ radical ions and neutral D_1 molecules: $D_1{\cdot}TDAE{\cdot}C_{60}$ †

Dmitri V. Konarev,*[a,b] Ivan S. Neretin,[c] Gunzi Saito,*[a] Yury L. Slovokhotov,[c] Akihiro Otsuka[a,d] and Rimma N. Lyubovskaya[b]

[a] *Division of Chemistry, Graduate School of Science, Kyoto University, Sakyo-ku, Kyoto 606-8502, Japan. E-mail: saito@kuchem.kyoto-u.ac.jp; Fax: +81-75-753-40-35*

[b] *Institute of Problems of Chemical Physics RAS, Chernogolovka, Moscow region 142432, Russia. E-mail: konarev@icp.ac.ru; Fax: +007-096-515-54-20*

[c] *Institute of Organoelement Compounds RAS, 28 Vavilov St., 119991, Moscow, Russia*

[d] *Research Center for Low Temperature and Materials Sciences, Kyoto University, Sakyo-ku, Kyoto 606-8502, Japan*

Received 29th May 2003, Accepted 8th August 2003
First published as an Advance Article on the web 3rd September 2003

New ionic complexes containing $TDAE^{\bullet+}$ and $C_{60}^{\bullet-}$ radical ions and neutral molecules: $(TBPDA)_2{\cdot}TDAE{\cdot}C_{60}$ (**1**); $CTV{\cdot}TDAE{\cdot}C_{60}$ (**2**); and $Co^{II}TPP{\cdot}TDAE{\cdot}C_{60}$ (**3**) (TDAE: tetrakis(dimethylamino)ethylene; TBPDA: *N,N,N′,N′*-tetrabenzyl-*p*-phenylenediamine; CTV: cyclotriveratrylene and $Co^{II}TPP$: tetraphenylporphyrinate cobalt (II)) were obtained as single crystals. The presence of $TDAE^{\bullet+}$, $C_{60}^{\bullet-}$ and neutral donors in **1**–**3** was proved by optical absorption spectra in the IR and UV-vis-NIR ranges. In the crystal structure of **1** studied by single crystal X-ray diffraction, $TDAE^{\bullet+}$ and $C_{60}^{\bullet-}$ are spatially separated by bulky TBPDA molecules. Magnetic susceptibilities of **1** and **2** follow the Curie–Weiss law with the negative Weiss temperatures (−2.3 and −2.0 K) and their magnetic moments decrease below 60 and 15 K, respectively. The EPR signals from **1** and **2** at the same temperatures are split into two components, which shift in the opposite directions to lower and higher fields with the temperature decrease. This phenomenon is explained by the formation of field-induced short-range magnetically ordered clusters. $Co^{II}TPP$ and $C_{60}^{\bullet-}$ form diamagnetic σ-bonded ($Co^{II}TPP{\cdot}C_{60}^{-}$) anions in **3** in the 1.9–190 K range. This allows one to observe the EPR signal from the isolated $TDAE^{\bullet+}$ radical cations (g = 2.0031 and halfwidth = ΔH = 3.22 mT at 4 K). Above 190 K the magnetic moment of **3** increases and the EPR signal is essentially broadened and shifted to a lager g-factor (g = 2.0194, ΔH = 24.2 mT at 290 K). This is attributed to the dissociation of the σ-bonded diamagnetic ($Co^{II}TPP{\cdot}C_{60}^{-}$) anions to non-bonded paramagnetic $Co^{II}TPP$ and $C_{60}^{\bullet-}$ components.

Introduction

Ionic compounds of fullerenes show intriguing physical properties including soft ferromagnetism in the C_{60} salt with tetrakis(dimethylamino)ethylene (TDAE) with T_c = 16.1 K[1] and the salt of chemically modified C_{60} with cobaltocene with T_c = 19 K.[2] The transition temperature in $TDAE{\cdot}C_{60}$ is the highest among those for all known nonpolymeric purely organic ferromagnets. To understand the origin of ferromagnetism in $TDAE{\cdot}C_{60}$ numerous magnetic, optical and structural investigations were carried out.[3,4] The transfer of one electron from TDAE to C_{60} followed by the formation of $TDAE^{\bullet+}$ and $C_{60}^{\bullet-}$ radical ions was proved by IR and Raman measurements on single crystals.[5,6] Magnetism in $TDAE{\cdot}C_{60}$ is attributed mainly to $C_{60}^{\bullet-}$ since the g-factor of the EPR signal at 2.0003[7] is close to that of $C_{60}^{\bullet-}$ (1.9991).[8] The EPR signal from $TDAE^{\bullet+}$ was not observed probably due to spin pairing.[9] The g = 2.0003 can also be considered as an intermediate value between those for $TDAE^{\bullet+}$ at 2.0035[10] and $C_{60}^{\bullet-}$ at 1.9991[8] due to the existence of strong exchange coupling between $TDAE^{\bullet+}$ and $C_{60}^{\bullet-}$[11] or the overlap of the EPR lines of $TDAE^{\bullet+}$ and $C_{60}^{\bullet-}$.[3] In this case $TDAE^{\bullet+}$ can also contribute to magnetism of this salt. The EPR study of $TDAE{\cdot}C_{60}$ single crystals showed antiferromagnetic exchange along the shortest crystallographic c-axis and spin canting in the orthogonal plane, which causes weak ferromagnetism along the a-axis below T_c.[12] This explanation is based on the Dzyaloshinsky–Moriya mechanism of long-range ferromagnetic ordering.[12] †

TDAE also forms ionic complexes with C_{70}.[13,14] Magnetic susceptibilities of these complexes follow the Curie–Weiss law. It was shown that there was no superexchange between $C_{70}^{\bullet-}$ across the TDAE methyl groups in $TDAE{\cdot}C_{70}$[13] and the diamagnetic $(C_{70}^{-})_2$ dimers were formed in $TDAE{\cdot}C_{70}{\cdot}C_6H_5Me$ (C_6H_5Me: toluene).[14] This could explain the absence of long-range magnetic ordering in C_{70} complexes with TDAE.

Up to now, $TDAE{\cdot}C_{60}$ has been considered to be the only ionic complex of fullerene that shows ferromagnetism. To design magnetic systems based on ionic complexes of fullerenes, chemically modified C_{60} may also be promising.[2] We developed a multi-component approach to the synthesis of ionic complexes of fullerenes with general composition $(D_1)(D_2^{\bullet+})(\text{fullerene}^{\bullet-})$, where D_1 is a large neutral molecule that forms a supramolecular packing pattern and D_2 is a donor molecule of a small size potentially able to reduce fullerene moiety. This approach afforded exotic fulleride compounds with the unusual diamagnetic σ-bonded ($Co^{II}TPP{\cdot}\text{fullerene}^{-}$) anions in $Co^{II}TPP{\cdot}[Cr^{I}(C_6H_6)_2]{\cdot}(\text{fullerene}){\cdot}C_6H_4Cl_2$ ($Cr(C_6H_6)_2$: bis(benzene)chromium; fullerenes: C_{60}, C_{70}, and $C_{60}(CN)_2$; $C_6H_4Cl_2$: *o*-dichlorobenzene)[15,16] and the diamagnetic $(C_{70}^{-})_2$ dimers in $CTV{\cdot}(Cs)_2{\cdot}(C_{70})_2{\cdot}(DMF)_7{\cdot}(C_6H_6)_{0.75}$ (CTV: cyclotriveratrylene; DMF: *N,N′*-dimethylformamide).[17] This method allows the investigation of the effect of incorporation of the neutral D_1 component (of different size, shape and electronic state) into ionic complexes on their magnetic and conductive properties.

In this study we used a strong organic donor TDAE as a D_2 component to obtain the complex containing $TDAE^{\bullet+}$ and $C_{60}^{\bullet-}$ radical ions together with neutral D_1 molecules. Three new ionic multi-component complexes $(TBPDA)_2{\cdot}TDAE{\cdot}C_{60}$ (**1**), $CTV{\cdot}TDAE{\cdot}C_{60}$ (**2**) and $Co^{II}TPP{\cdot}TDAE{\cdot}C_{60}$ (**3**) (TBPDA:

† Electronic supplementary information (ESI) available: The data of IR, UV-vis-NIR and EPR measurements of the starting compounds and complexes **1**–**3** (Tables S1–S3 and Fig. S1). See http://www.rsc.org/suppdata/dt/b3/b306074h/

DOI: 10.1039/b306074h

Table 1 The data for crystals of the complexes **1**–**3**

		Elemental analysis, found/calc.				
N	Complex	C (%)	H (%)	N (%)	[b]	Colour and shape
1	$(TBPDA)_2TDAE{\cdot}C_{60}$	86.10	4.54	5.61	3.75	Black prisms
		87.70	4.66	5.94		
2	$CTV{\cdot}TDAE{\cdot}C_{60}$ [a]	82.15	3.26	4.04	10.55	Black needles
		83.05	3.84	3.99		
3	$Co^{II}TPP{\cdot}TDAE{\cdot}C_{60}$ [a]	83.02	3.47	6.53	6.96	Black prisms
		84.31	3.20	6.89		

[a] According to IR data, **2** and **3** contain C_6H_6 solvent molecules. The elemental analysis indicates a small content of C_6H_6 and the compounds **2** and **3** were presented as $CTV{\cdot}TDAE{\cdot}C_{60}$ and $Co^{II}TPP{\cdot}TDAE{\cdot}C_{60}$. [b] 100% − (C, H, N)%.

N,N,N′,N′-tetrabenzyl-*p*-phenylenediamine; CTV: cyclotriveratrylene; $Co^{II}TPP$: tetraphenylporphyrinate cobalt (II)) were obtained (Scheme 1). The complexes were characterized by elemental analysis, IR, UV-vis-NIR spectra, EPR and SQUID measurements. The crystal structure of **1** was determined by a single crystal X-ray diffraction. The antiferromagnetic coupling in **1** and **2**, and the unusual transition from diamagnetic σ-bonded ($Co^{II}TPP{\cdot}C_{60}^{-}$) anions to paramagnetic non-bonded $Co^{II}TPP$ and $C_{60}^{\bullet-}$ components in **3** upon the increase of temperature are discussed. The properties of complexes **1**–**3** were compared with those of $TDAE{\cdot}C_{60}$.

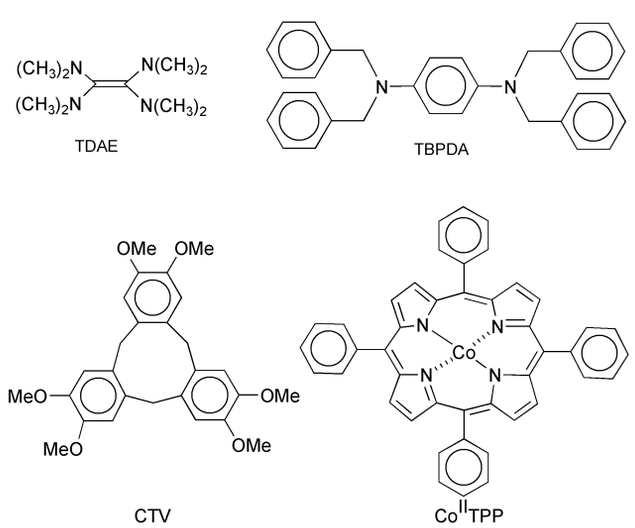

Scheme 1 Molecular components of the complexes.

Results and discussion

Synthesis

The complexes obtained are listed in Table 1. The common procedure for their preparation as single crystals is a slow diffusion of hexane into benzene/benzonitrile solution containing ionic $TDAE{\cdot}C_{60}$ in the presence of a neutral D_1 component. The important criterion for choosing the D_1 components is their ability to form stable ($D_1{\cdot}C_{60}$) complexes with neutral fullerene.[16,18–20] In several cases multi-component $D_1{\cdot}TDAE{\cdot}C_{60}$ crystallizes instead of two-component $TDAE{\cdot}C_{60}$. The shift of equilibrium from the two-component to the multi-component complex can be realized by using an excess of the D_1 component. The crystals of multi-component complexes, primarily identified by IR spectroscopy, were then studied by a whole set of physical methods mentioned above.

$(TBPDA)_2{\cdot}TDAE{\cdot}C_{60}$ (1), and $CTV{\cdot}TDAE{\cdot}C_{60}$ (2)

The IR spectra of **1** and **2** in KBr matrix are a superposition of those of $TDAE{\cdot}C_{60}$ [5] containing $TDAE^{\bullet+}$ and $C_{60}^{\bullet-}$ radical ions, and neutral TBPDA and CTV molecules whose bands are shifted by up to 10 cm^{-1} relative to parent ones. Starting C_{60} has four IR-active bands at 526, 576, 1182, 1429 cm^{-1} (the $F_{1u}(1–4)$ modes, respectively). The $F_{1u}(4)$ mode is shifted in **1** and **2** to 1389 and 1390 cm^{-1}, respectively, and the intensity of $F_{1u}(2)$ mode is essentially higher than that of the $F_{1u}(1)$ mode. These changes are characteristic of $C_{60}^{\bullet-}$.[21]

The presence of $C_{60}^{\bullet-}$ was supported by the characteristic absorption bands[22] at 10.7–10.8 (926–939 nm) and 9.2–9.3 × 10^3 cm^{-1} (1075–1087 nm) in the NIR spectra of **1** and **2** in KBr matrix. The additional bands in the IR and UV-vis-NIR ranges, which point to dimerization or polymerization of $C_{60}^{\bullet-}$,[23] were not observed indicating the monomeric state of $C_{60}^{\bullet-}$ in both complexes at room temperature (RT = 290 K).

Complex **1** crystallizes in a tetragonal system. The disordered C_{60} and TDAE molecules occupy 4/m symmetry, whereas the ordered TBPDA molecules are in 2/m positions. Fullerene anions are isolated from one another by the TBPDA molecules and packed in loose square layers parallel to the *ab*-plane (Fig. 1). The shortest distance between the centers of fullerene anions in the layer is equal to the unit cell parameters, $a = b =$ 13.626(2) Å, which is 3.5 Å larger than the C_{60}–C_{60} intercenter separation corresponding to van der Waals contacts between fullerenes.[24] Each TBPDA molecule contacts with hexagons of two C_{60} moieties by central phenylene fragments (indicating π-interaction) with $C(C_{60}) \cdots C(TBPDA)$ distances in the usual van der Waals range (3.43–3.68 Å). Disordered TDAE moieties are located within the layer in the voids formed by eight benzyl substituents of TBPDA (the shortest C(TBPDA) ··· C(TDAE) contacts are 3.63 Å). These voids alternate with fullerenes in a staggered order. The shortest distance between the centers of fullerenes and the midpoint of the central C=C bond of TDAE in the *ab*-plane is 9.63 Å. All intermolecular distances from C_{60} to C or N atoms of TDAE are

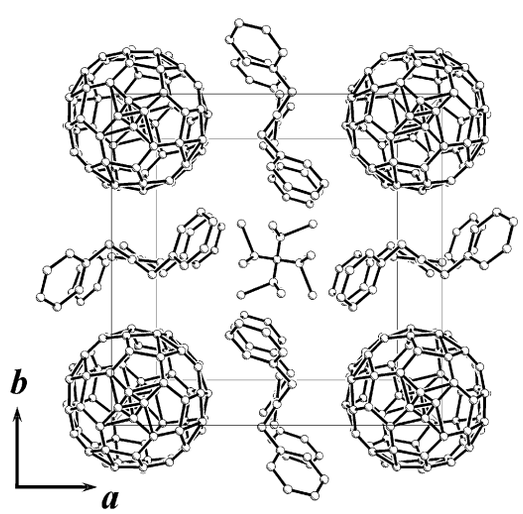

Fig. 1 View of the crystal structure of $(TBPDA)_2{\cdot}TDAE{\cdot}C_{60}$ (**1**) along the *c*-axis. Only one of two orientations of TDAE is shown.

longer than 5.5 Å (the sum of the van der Waals radii of two carbons or carbon and nitrogen atoms is 3.42 and 3.25 Å[25]). The similar C(TDAE) ··· C(C_{60}) contacts in TDAE·C_{60} are 3.40–3.48 Å.[26] The interlayer space is filled with the benzyl groups of TBPDA (Fig. 2).

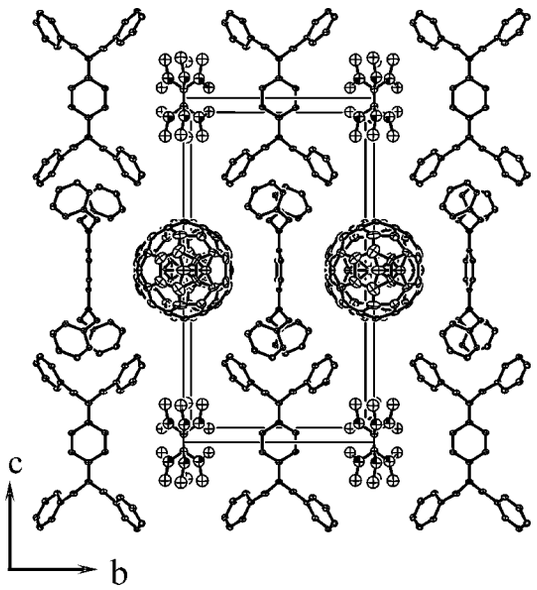

Fig. 2 View of the crystal structure of $(TBPDA)_2$·TDAE·C_{60} (**1**) along the *a*-axis.

The crystal structure of **1** viewed along the *a*-axis (Fig. 2) shows one-dimensional chains of alternating $TDAE^{\bullet+}$ and $C_{60}^{\bullet-}$ ions in the *c*-direction, separated from the neighboring ones by the TBPDA molecules. The distances between the centers of fullerenes and the midpoint of the central C=C bond of TDAE in this direction is 12.33 Å. Thus, the formation of **1** results in essential space separation of the $TDAE^{\bullet+}$ and $C_{60}^{\bullet-}$ radical ions by the neutral TBPDA molecules in all three directions.

The disorder of the TDAE molecule between two orientations does not allow one to discuss its bond distances and bond angles, which reflect a charged state of TDAE. The observed disorder pattern could result either from the overlapping of two planar ethylene moieties or from the overlapping of two moieties twisted by 90° about the C=C bond (Fig. 3). However, a planar conformation of TDAE leads to forbiddingly short Me ··· Me intramolecular contacts (down to 1.74 Å), so the TDAE moiety has a twisted conformation, which is characteristic of the TDAE cations.[5] The ordered TBPDA molecule retains its usual geometry[27] showing no participation in charge transfer. Torsion angles of the phenyl rings of the TBPDA molecule in **1** (70°) are slightly different from those of pristine TBPDA (85–87°)[27] probably due to packing forces.

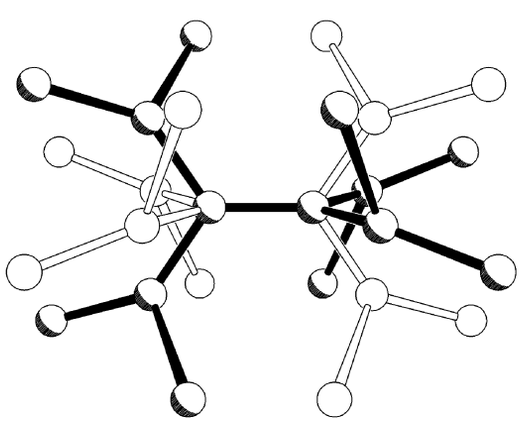

Fig. 3 Two orientations of disordered TDAE in $(TBPDA)_2$·TDAE·C_{60} (**1**).

The magnetic susceptibility of **1** at 60–300 K follows the Curie–Weiss law with the negative Weiss temperature (−2.3 K). The magnetic moment was estimated to be 1.97 μ_B at 300 K. This value is slightly larger than the calculated one for non-interacting $S = 1/2$ system (1.73 μ_B) and the magnetic moment of TDAE·C_{60}.[7] Below 60 K the magnetic moment of **1** decreases down to 1.5 μ_B at 1.9 K (Fig. 4) indicating the antiferromagnetic interaction of spins. Annealing the sample at 100 °C for 2 h does not change the magnetic behavior of **1**.

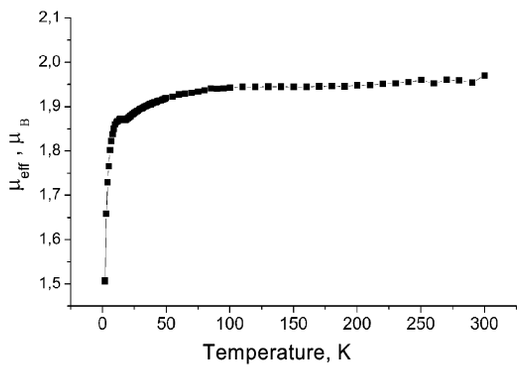

Fig. 4 The temperature dependence of magnetic moment of polycrystalline $(TBPDA)_2$·TDAE·C_{60} (**1**) between 1.9 and 300 K.

The EPR spectrum of **1** contains a single Lorentzian line with the *g*-factor of 2.0009 and the line half-width (ΔH) of 2.93 mT at RT. This *g*-factor is close to that of TDAE·C_{60} (the single line with the *g*-factor of 2.0003 and ΔH of 2.2 mT at RT[7]) and has a value between those for $TDAE^{\bullet+}$ of 2.0035[10] and $C_{60}^{\bullet-}$ of 1.9991.[8] Since strong exchange coupling between $TDAE^{\bullet+}$ and $C_{60}^{\bullet-}$ is not possible due to large space separation of these ions, the overlapping of the EPR lines of $TDAE^{\bullet+}$ and $C_{60}^{\bullet-}$ is possible. Indeed, the peak to peak separation between EPR lines of $TDAE^{\bullet+}$ and $C_{60}^{\bullet-}$ of about 0.7 mT is substantially smaller than ΔH of the EPR signal of **1** (about 3 mT).

The temperature dependences of the parameters of **1** are shown in Fig. 5. The *g*-factor of the signal remains almost

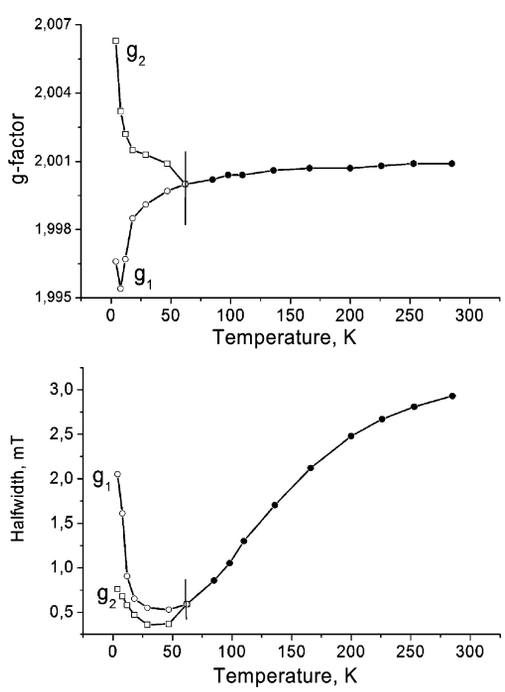

Fig. 5 The temperature dependence of *g*-factor (above) and ΔH (below) for the EPR signal of polycrystalline $(TBPDA)_2$·TDAE·C_{60} (**1**) between 4 and 290 K.

unchanged down to 60 K, whereas the line strongly narrows with the temperature decrease (ΔH = 0.5 mT at 60 K). A similar behavior of ΔH was observed in other solid ionic compounds of C_{60}.[22] The strong temperature dependence of ΔH seems to be an intrinsic property of $C_{60}^{\bullet -}$. Below 60 K the EPR signal becomes asymmetric and splits into two components, which shift symmetrically in opposite directions to higher and lower magnetic fields with the temperature decrease (g = 2.0068 and 1.9966 at 4 K, Fig. 5). The shifts are accompanied by a broadening of both components (ΔH = 2.05 and 0.76 mT at 4 K). The temperatures of the line splitting and the decrease of magnetic moment coincide indicating that splitting of the EPR signal originates from the antiferromagnetic interaction of spins. Such a behavior of **1** can be interpreted as a field-induced formation of short range magnetic clusters. It is interesting to note that the formation of these clusters was also observed both in C_{60} and C_{70} complexes with TDAE below 60 and 50 K.[28,13] In contrast to TDAE·$C_{60(70)}$, a direct magnetic interaction between $C_{60}^{\bullet -}$ or $C_{60}^{\bullet -}$ and $TDAE^{\bullet +}$ is not possible in **1** so their magnetic interaction probably occurs by an exchange mechanism through TBPDA molecules.

The magnetic behavior of **2** is qualitatively similar to that of **1**. Magnetic susceptibility follows the Curie–Weiss law with the −2.0 K Weiss temperature. The magnetic moment at RT is 1.78 μ_B and decreases below 15 K indicating an antiferromagnetic interaction of spins. The EPR signal from **2** is a single Lorentzian line with g = 2.0012 and ΔH = 1.76 mT at RT. The signal splits below 15 K into two components, shifted in opposite directions to higher and lower fields with the temperature decrease. As in **1**, the formation of field-induced short-range magnetic clusters is supposed in **2** below 15 K.

$Co^{II}TPP{\cdot}TDAE{\cdot}C_{60}$ (3)

$Cr^0(C_6H_6)_2$ was used earlier as a D_2 component to obtain the ionic multi-component complexes $Co^{II}TPP{\cdot}[Cr^I(C_6H_6)_2^{\bullet +}]{\cdot}$ (fullerene$^-$)·$C_6H_4Cl_2$ (fullerene: C_{60}, C_{70}, $C_{60}(CN)_2$) containing unusual diamagnetic σ-bonded ($Co^{II}TPP{\cdot}$fullerene$^-$) anions with short Co($Co^{II}TPP$) ··· C (fullerene) distances of 2.28–2.32 Å (Fig. 6).[15,16] The use of TDAE instead of $Cr^0(C_6H_6)_2$ results in the formation of $Co^{II}TPP{\cdot}TDAE{\cdot}C_{60}$ (**3**).

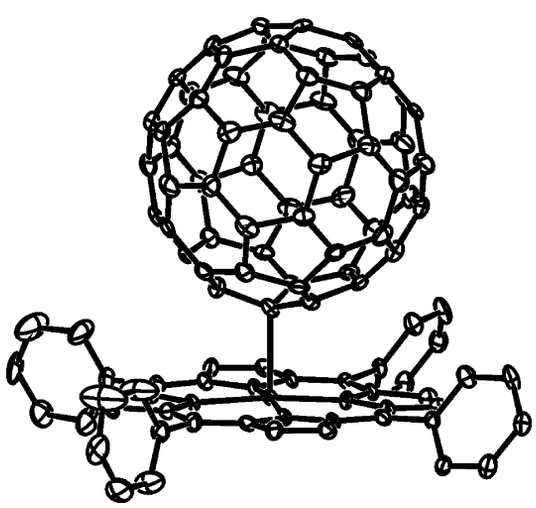

Fig. 6 View of the σ-bonded ($Co^{II}TPP{\cdot}C_{60}^-$) anion in $(Co^{II}TPP)_2{\cdot}[Cr^I(C_6H_6)_2]_{1.7}{\cdot}(C_{60})_2{\cdot}(C_6H_4Cl_2)_{3.3}$.[16]

The IR spectrum of **3** is a superposition of patterns from the $TDAE^{\bullet +}$ and $C_{60}^{\bullet -}$ radical ions and neutral $Co^{II}TPP$. The NIR spectrum of solid **3** contains a band of C_{60}^- at 9.2 × 10^3 cm^{-1} (1075 nm) together with an additional low-energy intense band at 7.7 × 10^3 cm^{-1} (1300 nm). The latter one was also observed upon the formation of $(Co^{II}TPP)_2{\cdot}[Cr^I(C_6H_6)_2]_{1.7}{\cdot}(C_{60})_2{\cdot}(C_6H_4Cl_2)_{3.3}$ containing the σ-bonded ($Co^{II}TPP{\cdot}C_{60}^-$) anions.[16] This band can be attributed to charge transfer between $Co^{II}TPP$ and C_{60}^- in one σ-bonded ($Co^{II}TPP{\cdot}C_{60}^-$) unit.[16]

The magnetic susceptibility of **3** follows the Curie–Weiss law with the Weiss temperature close to zero (0.2 K). Complex **3** formally contains three paramagnetic species with spin S = 1/2 ($Co^{II}TPP$, $TDAE^{\bullet +}$ and $C_{60}^{\bullet -}$), so the magnetic moment of 3 μ_B was expected. However, the observed magnetic moment is only 1.45 μ_B) in the 1.9–190 K range (Fig. 7). This value is even smaller than 1.73 μ_B calculated for S = 1/2 non-interacting system and corresponds to ~0.85 S = 1/2 spin per formula unit.

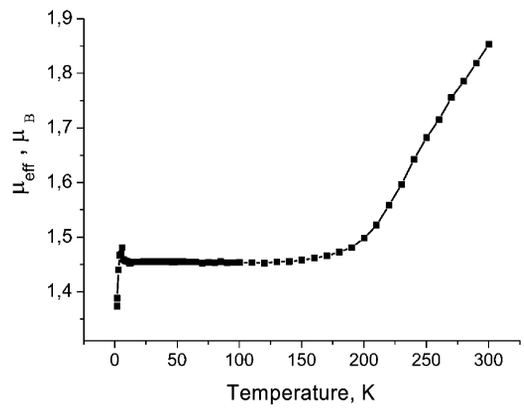

Fig. 7 The temperature dependence of the magnetic moment of polycrystalline $Co^{II}TPP{\cdot}TDAE{\cdot}C_{60}$ (**3**) between 1.9 and 300 K.

The EPR spectrum of **3** in the 4–190 K range is a single Lorentzian line with g = 2.0030–2.0050 and nearly constant ΔH of 3.2 mT (Fig. 8). This signal can be attributed to $TDAE^{\bullet +}$ (g = 2.0035[10]). Thus, ~0.85 spin per formula unit is localized mainly on $TDAE^{\bullet +}$ and the formation of diamagnetic ($Co^{II}TPP{\cdot}C_{60}^-$) anions in the 4–190 K range can be suggested. The presence of less than 1 spin per formula unit of **3** is probably due to the actual TDAE : C_{60} ratio also being less than 1: $Co^{II}TPP{\cdot}(TDAE)_x{\cdot}C_{60}$ (x < 1). However, the data of elemental analysis do not allow the exact determination of "x". Similarly in $(Co^{II}TPP)_2{\cdot}[Cr^I(C_6H_6)_2]_{1.7}{\cdot}(C_{60})_2{\cdot}(C_6H_4Cl_2)_{3.3}$, the $Cr^I(C_6H_6)_2$: C_{60} ratio determined by X-ray diffraction on a single crystal was 0.85.[16]

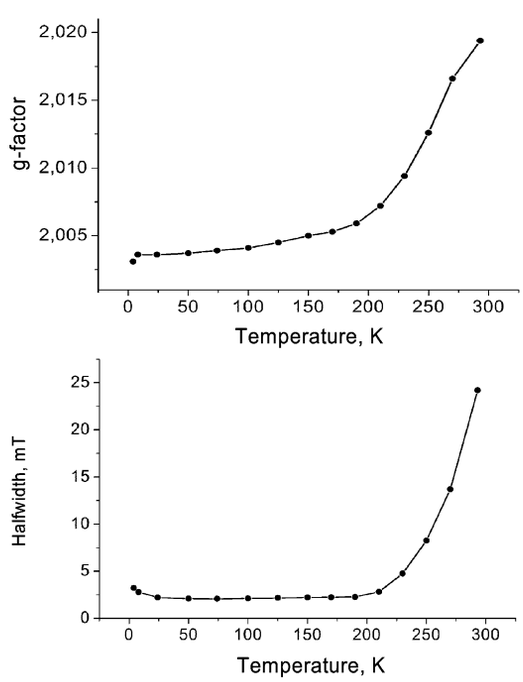

Fig. 8 The temperature dependence of the g-factor (above) and ΔH (below) for the EPR signal of polycrystalline $Co^{II}TPP{\cdot}TDAE{\cdot}C_{60}$ (**3**) between 4 and 290 K.

The formation of diamagnetic and EPR silent σ-bonded ($Co^{II}TPP{\cdot}C_{60}^{-}$) anions in **3** allow one to observe a separate EPR signal from $TDAE^{\bullet+}$ in contrast to the EPR spectra of **1** and **2**. Similarly, polymerization of $C_{60}^{\bullet-}$ in $TDAE{\cdot}C_{60}$ under 10 kbar pressure[29] or the formation of diamagnetic $(C_{70}^{-})_2$ dimers in $TDAE{\cdot}C_{70}{\cdot}C_6H_5Me$[14] result in the manifestation of EPR signal from $TDAE^{\bullet+}$.

Above 190 K the magnetic moment of **3** increases with temperature up to 1.85 μ_B at 300 K (Fig. 7) probably due to a contribution from the emerging paramagnetic $Co^{II}TPP$ and $C_{60}^{\bullet-}$ components (both have S = 1/2 ground state) into the total magnetic susceptibility of **3**. The increase of magnetic moment by 0.4 μ_B in the 190–300 K range corresponds to the contribution of 20% of total $Co^{II}TPP$ and $C_{60}^{\bullet-}$.

The appearance of a contribution from the paramagnetic $Co^{II}TPP$ and $C_{60}^{\bullet-}$ components is supported by EPR data. Above 190 K the signal essentially broadens and shifts to larger g-factors (g = 2.0194 and ΔH = 24.2 mT at RT) (Fig. 8). It is known that $Co^{II}TPP$ in complexes with neutral C_{60} and C_{70} shows a broad EPR signal with $g \cong 2.4$ and ΔH = 50–60 mT at RT.[24] Therefore, substantial broadening and a shift to larger g values of the EPR signal of **3** can be associated with the appearance of paramagnetic $Co^{II}TPP$ at higher temperatures. The presence of only one EPR signal instead of two or three in this sample indicates possible strong magnetic coupling between the paramagnetic species in **3**.

Diamagnetism observed for the ($Co^{II}TPP{\cdot}C_{60}^{-}$) anions below 190 K can be due to a direct participation of the HOMO of the C_{60}^{-} anions and d_{z^2} of $Co^{II}TPP$ in σ-bonding.[16] As was shown,[15,16] the σ-bond in the ($Co^{II}TPP{\cdot}C_{60}^{-}$) anions is rather weak (the Co ··· C bond length is 2.28–2.32 Å) as compared with the strong Co–C bond in alkylcobaltoamines (1.99–2.03 Å)[30] or the Co–N bond in CoTPP·NO (1.964 Å).[31,32] Because of this, dissociation of ($Co^{II}TPP{\cdot}C_{60}^{-}$) anions resulting in an additional contribution of their components to magnetic and spin susceptibility, is possible above 190 K. Such a transition is similar to dissociation of diamagnetic $(C_{70}^{-})_2$ and $(C_{60}^{-})_2$ dimers to paramagnetic $C_{70}^{\bullet-}$ and $C_{60}^{\bullet-}$ radical anions.[17,33,34]

$$\underset{\text{diamagnetic, EPR silent}}{\sigma\text{-bonded } (Co^{II}TPP \cdot C_{60}^{-})} \overset{190K}{\leftrightarrows} \underset{\text{paramagnetic, EPR active}}{\text{nonbonded } Co^{II}TPP \text{ and } C_{60}^{\bullet-}}$$

It is interesting to note that the small increase in the magnetic moments and the broadening of the EPR signals above 200 K were also observed in previously studied $(Co^{II}TPP)_2{\cdot}[Cr^{I}(C_6H_6)_2]_{1.7}{\cdot}(C_{60})_2{\cdot}(C_6H_4Cl_2)_{3.3}$ and $Co^{II}TPP{\cdot}[Cr^{I}(C_6H_6)_2]_2{\cdot}[C_{60}(CN)_2]_2{\cdot}(C_6H_4Cl_2)_3$.[15,16] These can also be attributed to the appearance of small contribution from non-bonded $Co^{II}TPP$ and $C_{60}^{\bullet-}$ or $C_{60}(CN)_2^{\bullet-}$. However, these effects are weaker in $Cr^{I}(C_6H_6)_2$ complexes than in **3** at RT.

Conclusion

New ionic complexes based on $TDAE^{\bullet+}$ and $C_{60}^{\bullet-}$ radical ions and neutral TBPDA, CTV, and $Co^{II}TPP$ molecules belonging to two different multi-component systems, have been obtained.

(1) The incorporation of two neutral and diamagnetic TBPDA molecules per ionic $TDAE{\cdot}C_{60}$ unit in $(TBPDA)_2{\cdot}TDAE{\cdot}C_{60}$ (**1**) spatially separates $TDAE^{\bullet+}$ and $C_{60}^{\bullet-}$ radical ions and yields a magnetically dilute system. This complex does not show ferromagnetic ordering of spins in contrast to $TDAE{\cdot}C_{60}$ but manifests the field-induced short-range antiferromagnetic ordering below 60 K, similar to pure $TDAE{\cdot}C_{60}$.[28] However, unlike $TDAE{\cdot}C_{60}$ where direct magnetic exchange between $TDAE^{\bullet+}$ and $C_{60}^{\bullet-}$ is possible, magnetic exchange in **1** is probably mediated by the TBPDA molecules. In $CTV{\cdot}TDAE{\cdot}C_{60}$ (**2**) the short range antiferromagnetic ordering is observed below 15 K.

(2) In crystalline $Co^{II}TPP{\cdot}TDAE{\cdot}C_{60}$ (**3**), isolated $TDAE^{\bullet+}$ radical cations and diamagnetic ($Co^{II}TPP{\cdot}C_{60}^{-}$) anions coexist below 190 K. The magnetic susceptibility of **3** shows paramagnetic behavior due to large spatial separation of $TDAE^{\bullet+}$ radical cations. It is shown that the EPR signal from $TDAE^{\bullet+}$ in **3** and related complexes may be revealed only in the presence of diamagnetic and EPR silent species like ($Co^{II}TPP{\cdot}C_{60}^{-}$). The contribution from non-bonded $Co^{II}TPP$ and $C_{60}^{\bullet-}$ appears above 190 K probably due to dissociation of σ-bonded diamagnetic ($Co^{II}TPP{\cdot}C_{60}^{-}$) anions to non-bonded paramagnetic $Co^{II}TPP$ and $C_{60}^{\bullet-}$ components.

Experimental

Materials

$Co^{II}TPP$ and TDAE were purchased from Aldrich, TBPDA from Lancaster, CTV from Acros and C_{60} of 99.98% purity from MTR Ltd.. Benzene (C_6H_6), hexane and benzonitrile (C_6H_5CN) (under reduced pressure) were distilled over Na/benzophenone in argon atmosphere. The solvents were degassed and stored in a glove box. All manipulations with **1**–**3** were carried out in a MBraun 150B-G glove box with controlled atmosphere and the content of H_2O and O_2 less than 1 ppm. The samples were stored in the glove box and were sealed in 2 mm quartz tubes for EPR and SQUID measurements under 10^{-5} Torr. KBr pellets for IR- and UV-vis-NIR measurements were prepared in the glove box.

Synthesis

Diffusion was carried out in a glass tube of 1.5 cm diameter and 40 mL volume with a ground glass plug for 1 month. The solvent was decanted and the crystals were washed with hexane and dried. The composition of **1** was determined from the X-ray diffraction on a single crystal and that of **1**–**3** by elemental analysis (Table 1). The difference in element content (100% − (C, H, N)%) for air-sensitive **1**–**3** indicates the addition of oxygen to the complex in the course of analysis (calc. one O_2 molecule per formula unit). The calculated C, H, and N (%) contents were corrected for this extrinsic oxygenation. Previously the addition of O_2 to ionic complexes of C_{60} during the elemental analysis was reported.[1,35]

The crystals of **1** were obtained by a slow diffusion of hexane (20 mL) in the 20 mL of C_6H_6/C_6H_5CN mixture (4:1) containing C_{60} (25 mg, 0.035 mmol), TDAE (0.05 mL) and TBPDA (160 mg, 0.34 mmol). The starting solution was prepared by dissolving C_{60} and TDAE in 4 ml of C_6H_5CN and stirring at 60 °C for 4 h, 16 ml of benzene was added, TBPDA was dissolved by stirring overnight at 60 °C, then the obtained solution was cooled down to the room temperature and filtered. After 1 month two types of crystals were formed, *viz*. large (up to 3 × 3 × 0.5 mm^3 size) black shiny prisms of **1** (70% yield) and small (up to 0.5 × 0.5 × 0.3 mm^3 size) brown crystals of **1** (20% yield), separated under a microscope. **1** is a ferromagnetic phase of $TDAE{\cdot}C_{60}$ according to IR and SQUID measurements.

The crystals of **2** were prepared similarly to **1**. C_{60} (25 mg, 0.035 mmol), TDAE (0.05 mL) and CTV (30 mg, 0.066 mmol) were used as starting reagents. The crystals of **2** grew as black thin needles (50% yield) with no admixture of $TDAE{\cdot}C_{60}$.

The crystals of **3** were obtained by the same procedure. C_{60} (25 mg, 0.035 mmol), TDAE (0.05 mL) and $Co^{II}TPP$ (20 mg, 0.030 mmol) were used as starting reagents. The crystals of **3** were obtained as black prisms with characteristic blue luster (70% yield). $TDAE{\cdot}C_{60}$ was not formed in the synthesis of **3**.

General

UV-vis-NIR spectra were measured on a Shimadzu-3100 spectrometer in the 240–2600 nm range. FT-IR spectra were measured in KBr pellets with a Perkin-Elmer 1000 Series spectrometer (400–7800 cm^{-1}). A Quantum Design MPMS-XL SQUID magnetometer was used to measure static susceptibilities between 300 and 1.9 K. A sample holder contribution and core temperature independent diamagnetic susceptibility (χ_0) were subtracted from the experimental values. The values of χ_0 were calculated for **1**–**3** from the high temperature range using the appropriate formula: $\chi_M = C/(T - \Theta;) + \chi_0$. EPR spectra were recorded down to 4 K with a JEOL JES-TE 200 X-band ESR spectrometer equipped with a JEOL ES-CT470 cryostat.

X-Ray crystal structure determination

Crystal data of **1**: $C_{138}H_{88}N_8$, M =1858.29, black prisms, tetragonal, space group $I4/m$. The unit cell parameters are: $a = b =$ 13.626(2), c = 24.662(5) Å, V = 4579.3(1) $Å^3$, Z = 2, D_c =1.348 g cm^{-3}, $F(000)$ = 1944.0.

X-Ray diffraction data were collected at 110 K on a Bruker SMART CCD diffractometer with an area detector (sealed tube, Mo Kα radiation, λ = 0.71073 Å, μ = 0.08 mm^{-1}). A series of three ω scans with a 0.3° frame width were collected. Reflection intensities were integrated using the SAINT program. In total, N_{tot} = 13250 reflections were measured up to $2\Theta_{max}$ = 60°, 2094 of them were independent. The structure was solved by direct methods using the SHELXTL program package [36] and refined by full-matrix least squares on F^2. The ordered non-hydrogen atoms were refined anisotropically. Hydrogen atoms were placed in calculated positions and refined within the 'riding atom' model. Fullerene molecules are disordered into two equally occupied positions related by the rotation about a two-fold crystallographic axis passing through the midpoints of two oppositely located 6–6 bonds. The TDAE molecule is also disordered between two orientations with equal occupancy. The least-square refinement on F^2 was done to R_1 = 0.1002 for 1150 observed reflections with $F > 4\sigma(F)$, wR_2 = 0.330 (213 parameters), final GoF = 1.040.

CCDC reference number 211611.

See http://www.rsc.org/suppdata/dt/b3/b306074h/ for crystallographic data in CIF or other electronic format.

Acknowledgements

The work was supported by the COE Research on Elements Science 12CE2005, JSPS, and the RFBR grants N 03-03-32699a and 02-03-33225a.

References

1 P.-M. Allemand, K. C. Khemani, A. Koch, F. Wudl, K. Holczer, S. Donovan, G. Grüner and J. D. Thompson, *Science*, 1991, **253**, 301.
2 D. Mihailovic, *Monatsh. Chem.*, 2003, **134**, 137.
3 B. Gotschy, *Fullerene Sci. and Technol.*, 1996, **4**, 677.
4 B. Narymbetov, A. Omerzu, V. V. Kabanov, M. Tokumoto, H. Kobayashi and D. Mihailovic, *Nature*, 2000, **407**, 883.
5 K. Pokhodnia, J. Papavassiliou, P. Umek, A. Omerzu and D. Mihailovic, *J. Phys. Chem.*, 1999, **110**, 3606.
6 K. Pokhodnia, J. Demsar, A. Omerzu, D. Mihailovic and H. Kuzmany, *Phys. Rev. B*, 1997, **55**, 3762.
7 K. Tanaka, A. A. Zakhidov, K. Yoshizawa, K. Okahara, T. Yamabe, K. Yakushi, K. Kikuchi, S. Suzuku, L. Ikemoto and Y. Achiba, *Phys. Rev. B*, 1993, **47**, 7554.
8 P.-M. Allemand, G. Srdanov, A. Koch, K. Khemani, F. Wudl, Y. Rubin, F. Diederich, M. M. Alvarez, S. J. Anz and R. L. Whetten, *J. Am. Chem. Soc.*, 1991, **113**, 2780.
9 R. Blink, D. Arcon and K. Pokhodnya, *Synth. Met.*, 1997, **85**, 1713.
10 K. Kuwata and D. H. Geske, *J. Am. Chem. Soc.*, 1964, **86**, 2101.
11 B. Gotschy, R. Gompper, H. Klos, A. Schilder, W. Schütz and G. Völkel, *Synth. Met.*, 1996, **77**, 287.
12 R. Blink, K. Pokhodnia, P. Cevc, D. Arcon, A. Omerzu, D. Mihailovic, P. Venturini, L. Golic, Z. Trontelj, J. Luznik, Z. Jeglicic and J. Pirnat, *Phys. Rev. Lett.*, 1996, **76**, 523.
13 D. Arcon, R. Blinc, P. Cevk, G. Chouteau and A.-L. Barra, *Phys. Rev. B*, 1997, **56**, 10786.
14 K. Oshima, T. Kambe, M. Fujiwara and Y. Nogami, *Synth. Met.*, 2003, **133–134**, 609.
15 D. V. Konarev, S. S. Khasanov, A. Otsuka, Y. Yoshida and G. Saito, *J. Am. Chem. Soc.*, 2002, **124**, 7648.
16 D. V. Konarev, S. S. Khasanov, A. Otsuka, Y. Yoshida, R. N. Lyubovskaya and G. Saito, *Chem. Eur. J.*, 2003, **9**, 3837.
17 D. V. Konarev, S. S. Khasanov, I. I. Vorontsov, G. Saito, Yu. A. Antipin, A. Otsuka and R. N. Lyubovskaya, *Chem. Commun.*, 2002, 2548.
18 D. V. Konarev, A. Yu. Kovalevsky, A. L. Litvinov, N. V. Drichko, B. P. Tarasov, P. Coppens and R. N. Lyubovskaya, *J Solid State Chem.*, 2002, **168**, 474.
19 J. L. Atwood, M. J. Barnes, M. G. Gardiner and C. L. Raston, *Chem. Commun.*, 1996, 1449.
20 D. V. Konarev and R. N. Lyubovskaya, *Russ. Chem. Rev.*, 1999, **68**, 19.
21 T. Picher, R. Winkler and H. Kuzmany, *Phys. Rev. B*, 1994, **49**, 15879.
22 C. A. Reed and R. D. Bolskar, *Chem. Rev.*, 2000, **100**, 1075.
23 M. S. Dresselhaus and G. Dresselhaus, in *Fullerene Polymers and Fullerene Polymer Composites,* ed. P. C. Eklund and A. M. Rao, Springer-Verlag, Berlin, 1999, pp. 1–58.
24 D. V. Konarev, I. S. Neretin, Yu. L. Slovokhotov, E. I. Yudanova, N. V. Drichko, Yu. M. Shul'ga, B. P. Tarasov, L. L. Gumanov, A. S. Batsanov, J. A. K. Howard and R. N. Lyubovskaya, *Chem. Eur. J.*, 2001, **7**, 2605.
25 Yu. V. Zefirov and P. M. Zorkii, *Russ. Chem. Rev.*, 1995, **64**, 415.
26 B. Narymbetov, H. Kobayashi, M. Tokumoto, A. Omerzu and D. Mihailovic, *Chem. Commun.*, 1999, 1511.
27 C. Rickert, M. Pirotta and T. Muller, *Acta Crystallogr., Sect. C*, 1992, **48**, 2233.
28 A. L. Maneiro, L. Pasimeni, L. C. Brunel, L. A. Pardi, G. Cao and R. P. Guertin, *Solid State Commun.*, 1998, **106**, 727.
29 K. Mizoguchi, M. Machino, H. Sakamoto, M. Tokumoto, T. Kawamoto, A. Omerzu and D. Mihailovic, *Synth. Met.*, 2001, **121**, 1778.
30 M. Rossi, J. P. Glusker, L. Randaccio, M. F. Summers, P. J. Toscano and L. G. Marzilli, *J. Am. Chem. Soc*, 1985, **107**, 1729.
31 B. B. Wayland, J. V. Minkiewicz and M. E. Abd-Elmageed, *J. Am. Chem. Soc.*, 1974, **96**, 2795.
32 W. R. Scheidt and J. L. Hoard, *J. Am. Chem. Soc.*, 1973, **95**, 8281.
33 D. V. Konarev, S. S. Khasanov, A. Otsuka and G. Saito, *J. Am. Chem. Soc.*, 2002, **124**, 8520.
34 A. Hönnerscheid, L. Wüllen, M. Jansen, J. Rahmer and M. Mehring, *J. Chem. Phys.*, 2001, **115**, 7161.
35 T. Kitagawa, Y. Lee and K. Takeuchi, *Chem. Commun.*, 1999, 1529.
36 SHELXTL, An integrated system for solving, refining and displaying crystal structures from diffraction data, Version 5.10, Bruker Analytical X-ray Systems, Madison, WI, USA, 1997.